

Characterization of Boria–Alumina Mixed Oxides Prepared by a Sol–Gel Method. 2. Characterization of the Calcined Xerogels

Franck Dumeignil,[†] Monique Rigole, Michel Guelton, and Jean Grimblot*

Laboratoire de Catalyse de Lille, UMR CNRS 8010, Université des Sciences et Technologies de Lille, Bâtiment C3, 59655 Villeneuve d'Ascq Cedex, France

Received November 2, 2004. Revised Manuscript Received February 9, 2005

Sol–gel boria–alumina mixed oxides with a wide range of B/Al atomic compositions have been characterized as dried xerogels in the preceding paper in which a structural model with four domains of composition was proposed. The present paper presents the results obtained on the same series of solids after calcination at 500 °C. It was found that the structure of the dried xerogels has a strong influence on the structure of the final oxides. In particular, in the dried xerogel state from B/Al \approx 0.15, BO₃ chains crossed over the solid matrix, and this ratio was also a crucial limit for the calcined solids structure. Indeed, during calcination some BO₃ chains were volatilized, giving a measured B/Al ratio lower than the theoretical one; the oxides were dislocated and their SSA brutally increasing from \sim 500 m²·g^{−1} up to \sim 650 m²·g^{−1}. Cleavage resulted in the exposition of new external surfaces that exhibited BO₃OH species incrustated in the host alumina matrix, conferring then an epitactic character to the solids. Further, the ¹¹B magic-angle spinning (MAS) NMR spectra of the solids exhibited a feature constituted of BO₃ and BO₄ (hydrated surface BO₃ species) components that were resolved by a software simulation. While for B/Al < 0.15 the quadrupolar interaction on the BO₄ species was of about 0.4 MHz, it increased up to about 0.9 MHz for B/Al > 0.15. This increase originated in a strain on the new BO₃ species trapped along the cleaved surfaces. Further, X-ray diffraction and X-ray photoelectron spectroscopy results showed that, while for B/Al < 0.15, the system can be considered as an alumina matrix locally modified by insertion of BO₃ species, for B/Al > 0.15 a mixed phase was progressively formed. In good agreement, the ²⁷Al MAS NMR spectra of the solids with high B/Al ratio were similar to that expected for model boria–alumina mixed phases. In addition, the BO₄/BO₃ ratios calculated by simulation of the ¹¹B MAS NMR spectra were consistent with the XPS results. We calculated the proportion of B species (in wt %) present on the surface of the solids (i.e., BO₄ species), which can be potentially involved in catalytic reactions. It was remarkable that the tendency observed for the BO₄ wt % as a function of the B/Al ratio was consistent with a boria–alumina phase diagram previously proposed by Giellisse et al.

Introduction

As we previously reported,¹ different boria–alumina mixed oxides have been widely used for catalytic applications by themselves^{2–25} or as supports for various active phases^{26–31} or more specifically as supports for hydrotreating catalysts.^{32–53}

Nevertheless, the structure of the boria–alumina system with high specific surface areas is not yet satisfactory described and the present work aims at proposing a detailed analysis of B₂O₃–Al₂O₃ carriers prepared by an original sol–gel

* To whom correspondence should be addressed. E-mail: jean.grimblot@ensc-lille.fr.

[†] Present address: Department of Chemical Engineering, Tokyo University of Agriculture and Technology, 2-24-16 Nakacho, Koganei, Tokyo 184-8588, Japan.

- (1) Dumeignil, F.; Guelton, M.; Rigole, M.; Grimblot, J. *Chem. Mater.* **2005**, *17*, 2361–2368.
- (2) Curtin, T.; McMonagle, J. B.; Hodnett, B. K. *Appl. Catal., A* **1992**, *93*, 91.
- (3) Izumi, Y.; Sato, S.; Urabe, K. *Chem. Lett.* **1983**, 1649.
- (4) Curtin, T.; McMonagle, J. B.; Hodnett, B. K. *Appl. Catal., A* **1992**, *93*, 75.
- (5) Werke, L. East German Patent 10,920, 1955.
- (6) Irnich, R.; BASF, German Patent 1,227,028, 1976.
- (7) Immel, O.; De Jager, A.; Kaiser, B.-U.; Schwarz, H.-H. Bayer, Jpn. Patent S53-037686, 1978.
- (8) Murakami, Y.; Saeki, Y.; Ito, K. *Nippon Kagaku Kaishi* **1972**, *1*, 12.
- (9) Sakurai, H.; Sato, S.; Urabe, K.; Izumi, Y. *Chem. Lett.* **1985**, 1783.
- (10) Delmastro, A.; Gozzelino, G.; Mazza, D.; Vallino, M.; Busca, G.; Lorenzelli, V. *J. Chem. Soc., Faraday Trans.* **1994**, *90*, 2663.
- (11) Wang, W. J.; Che, Y. W. *Catal. Lett.* **1991**, *10*, 297.
- (12) Peil, K.; Galya, L. G.; Marcelin, G. *J. Catal.* **1989**, *115*, 441.
- (13) Engels, S.; Herold, E.; Lausch, H.; Mayr, H.; Meiners, H. W.; Wilde, M. *Proceedings of the 10th International Congress on Catalysis*; Budapest, Hungary, 19–24 July, 1992, 2581.

- (14) Murakami, Y.; Otsuka, K.; Wada, Y.; Morikawa, A. *Bull. Chem. Soc. Jpn.* **1990**, *63*, 340.
- (15) Cucinieri-Colorio, G.; Auroux, A.; Bonnetot, B. *J. Therm. Anal.* **1993**, *40*, 1267.
- (16) Cucinieri-Colorio, G.; Bonnetot, B.; Védrine, J. C.; Auroux, A. *New Developments in Selective Oxidation*; Cortés Corberán, V., Bellón, S. V., Eds.; Elsevier Science Publishers: Amsterdam, 1994, 143.
- (17) Colorio, G.; Védrine, J. C.; Auroux, A.; Bonnetot, B. *Appl. Catal., A* **1996**, *137*, 55.
- (18) Buyevskaya, O. V.; Kubik, M.; Baerns, M. *Symposium on Heterogeneous Hydrocarbon Oxidation Presented before the Division of Petroleum Chemistry, Inc., 211th National Meeting*; American Chemical Society: New Orleans, LA, 24–29 March, 1996, 163.
- (19) Pine, L. U.S. Patent 3,993,557, 1976.
- (20) Bailey, W. A. *US Patent* 2377744, 1945.
- (21) De Bataafsche, N. V.; Petroleum Maatschappij, te's-Gravenhage. Dutch Patent 62,287, 1949.
- (22) De Bataafsche, N. V.; Petroleum Maatschappij, te's-Gravenhage. Dutch Patent 65,287, 1950.
- (23) Sato, S.; Kuroki, M.; Sodesawa, T.; Nozaki, F.; Maciel, G. E. *J. Mol. Catal. A: Chem.* **1995**, *104*, 171.
- (24) Izumi, Y.; Shiba, T. *Bull. Chem. Soc. Jpn.* **1964**, *37*, 7 n°12, 1797.
- (25) Tanabe, K. *Solid Acids and Bases, their catalytic properties*; Academic Press: New York-London, 1970; p 131.
- (26) Xiaoding, X.; Boelhouwer, C.; Bencke, J. I.; Vonk, D.; Mol, J. C. *J. Chem. Soc., Faraday Trans. 1* **1986**, *82*, 1945.

method. In a preliminary study, the structure of solids with low boron loadings⁵⁴ ($B/Al < 0.14$) was elucidated and it was decided to further extend the investigation to a wider range of B/Al compositions. In the preceding paper,¹ the structure of the dried solids prepared by a sol–gel synthesis method (xerogels) with a wide range of B/Al atomic composition (from 0 up to 1.643) was described. This first study was carried out by interpreting the ¹¹B and ²⁷Al spectra obtained by solid-state magic angle spinning (MAS) NMR spectroscopy. The results suggested that the structure of the solids depends on the B/Al atomic ratio and four domains have been identified:

(1) In domain I ($B/Al < 0.06$), matrix and surface tetrahedral aluminum species were created in addition to the usually observed octahedral aluminum species of the host boehmite structure. For $B/Al = 0.06$, 1% of the aluminum species were in a tetrahedral coordination surrounded by 4 boron oxo-species.

(2) In domain II ($0.06 < B/Al < 0.15$), new tetrahedral aluminum species were not created; BO₃ chains started to develop from the tetrahedral aluminum species already present in domain I.

(3) In domain III ($0.15 < B/Al < 0.48$), the BO₃ ribbons progressively crossed over the boehmite matrix and emerged on its surface leading to the creation of new surface tetrahedral aluminum species at their ends. These new surface aluminum tetrahedral species became nucleation points of

new BO₃ chains. Further, supposedly due to particularly strong strains, some tetrahedral alumina species were converted into pentahedral aluminum species.

(4) In domain IV ($B/Al > 0.45$), the new BO₃ chains further developed into the host matrix.

The above-described model, built by interpreting NMR results, fits very well with the results of various characterization techniques presented in the present paper for the solids of the same origin but after calcination in air. Indeed, in addition to the use of solid-state MAS NMR spectroscopy, specific surface area measurements, X-ray diffraction (XRD), X-ray photoelectron spectroscopy (XPS), and atomic composition determination permitted to thoroughly characterize the calcined mixed oxides, the calcination stage being necessary to convert the boron modified boehmite phase into a catalytically utilizable boron modified γ -alumina (B₂O₃–Al₂O₃) support. The results of the various techniques matched up very well each other, and it was demonstrated that the final structure of the calcined mixed oxides strongly depended on the initial structure of the dried xerogels from which they are issued.

Experimental Section

Mixed Oxides Synthesis. The boria–alumina supports were synthesized according to an original sol–gel method described elsewhere.^{1,54} After hydrolysis, stirring, and drying, the obtained dried xerogels¹ were further calcined for 3 h in flowing air at 500 °C, this temperature being reached at a rate of 40 °C·h^{−1}.

Sample Compositions. Bulk atomic composition of the calcined samples was determined at the Service Central d'Analyses du CNRS (Vernaison, France) by X-ray fluorescence. The objectives of these analyses were to compare the actual compositions of the calcined oxides with the theoretical ones.

XRD. A Siemens D 5000 diffractometer equipped with a copper anode and a secondary monochromator, whose tension was adjusted at 50 kV (35 mA), was used. The sample was deposited at room temperature on a glass disk placed on a rotating holder in order to avoid eventual preferential orientations. The X-ray beam, emitted by a fixed source, reached the sample rotating around its holder axis. By reflection, the diffracted beam was detected by a scintillation counter. A diffraction angle of θ corresponded a 2θ moving of the counter on the diffractometer circle. The recordings were made with a measure step of 0.2° in a domain from $2\theta = 5^\circ$ to $2\theta = 75^\circ$ and with an integration time of 30 s.

XPS. The spectra were recorded on an AEI ES200B spectrometer. The X-ray source was an aluminum anode ($E = 1486.6$ eV) excited under a power of 300 W (12 kV, 25 mA). The samples were grinded in an agate mortar and then pressed on indium before being introduced in the analysis chamber under a vacuum inferior to 4×10^{-8} Torr. The obtained information was both qualitative and quantitative.⁵⁵ Further, the three-dimensional thick binary oxide model⁵⁵ was used to interpret spectra intensity variations as it is suitable and very convenient to characterize bulk samples prepared by the sol–gel method. This model allows following the boron distribution (or repartition) within the alumina matrix.

NMR. MAS NMR. Similar to the xerogels,^{1,54} the MAS NMR spectroscopy was used in order to characterize the local environment of the aluminum and boron species in/on the calcined samples. The spectra were recorded on a Bruker ASX 400 spectrometer working

- (27) Sibeijn, M.; van Veen, J. A. R.; Blik, A.; Moulijn, J. A. *J. Catal.* **1994**, *145*, 416.
- (28) Chen, Y. W.; Li, C. *Catal. Lett.* **1992**, *13*, 359.
- (29) Nadirov, N. K.; Vozdvizhenskii, V. F.; Kondratkova, N. I.; Fatkulina, A. A. *React. Kinet. Catal. Lett.* **1985**, *27* (1), 191.
- (30) Peil, K. P.; Galya, L. G.; Marcelin, G. *Catalysis: Theory to Practice. 9th International Congress on Catalysis*; Canada, 1988, 1712.
- (31) Okihara, T.; Tamura, H.; Misono, M. *J. Catal.* **1995**, *95*, 41.
- (32) de Rosset, A. J. U.S. Patent 2,938,001, 1960.
- (33) O'Hara, M. J. U.S. Patent 3,453,219, 1969.
- (34) Plundo, R. A. U.S. Patent 3,617,532, 1971.
- (35) Dufresne, P.; Marcilly, C. Fr. Patent 2,561,945, 1985.
- (36) Pine, L. A. U.S. Patent 3,954,670, 1976.
- (37) O'Hara, M. J. U.S. Patent 3,525,684, 1970.
- (38) O'Hara, M. J. U.S. Patent 3,666,685, 1972.
- (39) Polard, R. J.; Voorhies, J. D. U.S. Patent 4,139,492, 1979.
- (40) Toulhoat, H. Eur. Patent 0,297,949, 1989.
- (41) Morishige, H.; Akai, Y. *Bull. Soc. Chim. Belg.* **1995**, *104* (4–5), 253.
- (42) Stranick, M. A.; Houalla, M.; Hercules, D. M. *J. Catal.* **1987**, *104*, 396.
- (43) Houalla, M.; Delmon, B. *Appl. Catal.* **1981**, *1*, 285.
- (44) Vorob'ev, V. N.; Agzamkhodzhaeva, D. R.; Mikita, V. P.; Abidove, M. F. *Kinetika i Kataliz* **1984**, *25*, 154.
- (45) Ramírez, J.; Castillo, P.; Cedeño, L.; Cuevas, R.; Castillo, M.; Palacios, J. M.; López-Agudo, A. *Appl. Catal., A* **1995**, *132*, 317.
- (46) Li, C.; Chen, Y. W.; Yang, S. J.; Wu, J. C. *Ind. Eng. Chem. Res.* **1993**, *32*, 1573.
- (47) Tsai, M. C.; Chen, Y. W.; Kang, B. C.; Wu, J. C.; Leu, L. J. *Ind. Eng. Chem. Res.* **1991**, *30*, 1801.
- (48) Chen, Y. M.; Tsai, M. C.; Kang, B. C.; Wu, J. C. *AIChE Summer National Meeting*, 1990, 101.
- (49) Dubois, J. L.; Fujieda, S. *Catal. Today* **1996**, *29*, 191.
- (50) Muralidhar, G.; Massoth, F. E.; Shabtai, J. *J. Catal.* **1984**, *85*, 44.
- (51) Li, D.; Sato, T.; Imamura, M.; Shimada, H.; Nishijima, A. *J. Catal.* **1997**, *170*, 357.
- (52) Lafitau, H.; Neel, E.; Clement, J. C. *Preparation of Catalysts*; Delmon, B., Jabobs, P. A., Poncelet, J., Eds.; Elsevier Scientific Publishing Company: Amsterdam, 1976, 393.
- (53) Mertens, F. P.; Dai, E. P.; Bartley, B. H.; Neff, L. D. *Symposium on Advances in Hydrotreating Catalysts Presented before the Division of Petroleum Chemistry Inc., 208th National Meeting*; American Chemical Society: Washington D.C., August 1994, 1–26, 566.
- (54) Dumeignil, F.; Guelton, M.; Rigole, M.; Amoureux, J. P.; Fernandez, C.; Grimblot, J. *Colloids Surf. A* **1998**, *158* (1), 75.

- (55) Grimblot, J. *L'analyse de surface des solides par spectroscopies électroniques et ioniques*; Masson: Paris, 1995.

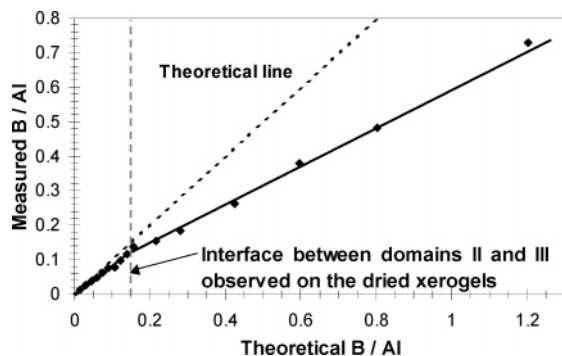


Figure 1. Measured B/Al atomic ratio in the calcined oxides as a function of the theoretical one (xerogel composition).

at 104.229 MHz (^{27}Al) and 128.33 MHz (^{11}B). The ^{27}Al spectra were recorded at a rotation frequency of 15000 Hz, with a pulse length of 0.8 μs and a repetition time between two acquisitions of 3 s; the reference at 0 ppm was taken for $\text{Al}(\text{H}_2\text{O})_6^{3+}$. The ^{11}B spectra were recorded with a rotation frequency of 14500 Hz, with a pulse length of 10 μs and a repetition time of 10 s, the reference at 0 ppm being taken for $\text{BF}_3\cdot\text{OEt}_2$.

MQ-MAS NMR. To confirm the assignment of the aluminum species peaks (in particular of the pentahedral aluminum species), a MQ-MAS NMR spectra (2D NMR) was recorded using an experimental method described elsewhere.⁵⁶

Brunauer–Emmett–Teller (BET) Specific Surface Area (SSA) Measurements. The SSAs of the calcined oxides were determined using the one-point BET method on a Quantasorb Junior (Ankersmit) after degassing the samples under primary vacuum at 250 °C for 2 h.

Results and Discussion

Composition of the Oxides. The B/Al atomic ratios, determined by X-ray fluorescence, are reported in Figure 1 as a function of the theoretical ones (ratios used during the sol–gel synthesis). Up to $\text{B/Al} \approx 0.15$, the measured B/Al ratio was equal to the expected one. In contrast, at higher B loadings ($\text{B/Al} > 0.15$), the measured B/Al ratios of the calcined oxides became significantly less than the theoretical ones. It is remarkable that this transition ratio ($\text{B/Al} = 0.15$) corresponds to the limit between domains II and III, as defined for the dried xerogels.¹ Indeed, in the dried xerogels, when the B/Al ratio was higher than 0.15, the results suggested that BO_3 chains started to emerge from the host matrix, progressively dislocating the boehmite mother structure. In addition it has been previously observed several times that, near 500 °C, boron oxides or polymeric BO_3 like chains are volatile,^{14,57,58} in good agreement with the Giellisse et al. diagram⁵⁹ (Figure 2) that shows that B_2O_3 is fusible near 470 °C. Therefore, the results presented in Figure 1 suggest that a part of the boron oxo-species present as BO_3 chains of different lengths in the xerogels volatilizes during the calcination step at 500 °C. Then, the actual B/Al ratio becomes inferior to the desired one. Note that when $\text{B/Al} >$

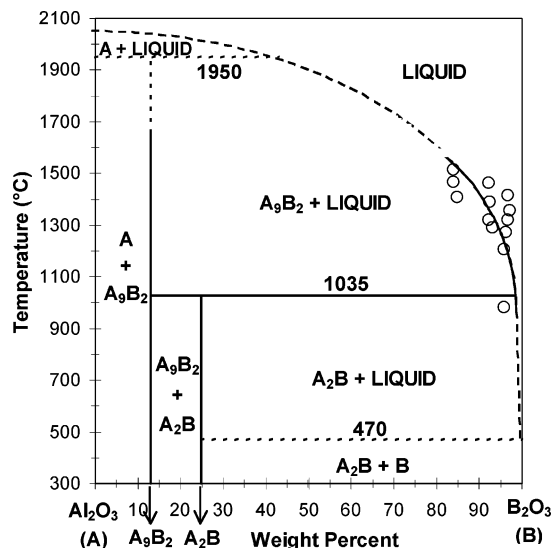


Figure 2. Giellisse et al. phase diagram (adapted from ref 59). A = Al_2O_3 , B = B_2O_3 , $\text{A}_9\text{B}_2 = 9\text{Al}_2\text{O}_3\cdot 2\text{B}_2\text{O}_3$, $\text{A}_2\text{B} = 2\text{Al}_2\text{O}_3\cdot \text{B}_2\text{O}_3$.

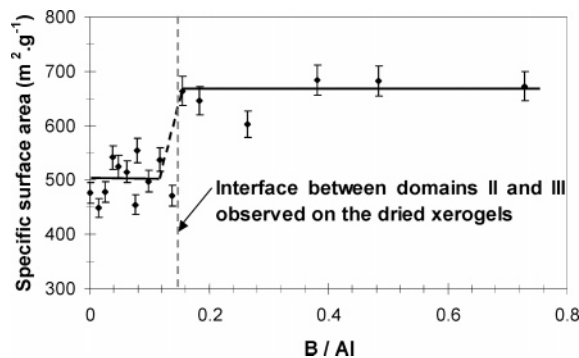


Figure 3. Specific surface areas of the calcined samples.

0.15, the BO_3 chains in the xerogels are sufficiently long for crossing the host matrix. The value of 0.15 for the B/Al ratio seems to be a key value for this kind of solids as all the characterization techniques used later in the present work exhibit a change of behavior from this ratio.

Texture of the Solids (SSA). The SSAs of the calcined oxides are reported in Figure 3. While the SSAs are constant at a value of about 500 $\text{m}^2\cdot\text{g}^{-1}$ up to $\text{B/Al} = 0.15$, a clear and net increase is observed for higher boron loadings, for which the SSAs are about 650 $\text{m}^2\cdot\text{g}^{-1}$, irrespective of the boron amount. As recalled above, this 0.15 value corresponds to the beginning of domain III in the xerogels. From this ratio, BO_3 chains start to crossover the boehmite matrix. Then, the boehmite host structure is progressively dislocating by the BO_3 chains development. In addition, as the BO_3 chains (partly) volatilize during the calcination step (B deficit observed in Figure 1 for $\text{B/Al} > 0.15$), further dismembering of the solid structure during calcination with formation of smaller particles can explain such a SSA increase.

Structure. XRD. The X-ray diffractograms of the calcined mixed oxides are presented in Figure 4. In addition, in Table 1 are gathered the characteristic features of standard boron and boron–aluminum oxides that might be formed. Unfortunately, it is quite difficult to unambiguously interpret the diffractograms of Figure 4 as the solids appear to be poorly crystallized, with rather weak and broad peaks. Thus, the

(56) Quartararo, J.; Amoureux, J.-P.; Grimblot, J. *J. Mol. Catal., A* **2000**, 162 (1–2), 353.

(57) Curtin, T.; McMonagle, J. B.; Hodnett, B. K. *Heterogeneous Catalysis and Fine Chemicals II*; Guisnet, M.; Barrault, J.; Bouchoule, C.; Duprez, D.; Pérot, G., Eds.; Elsevier: Amsterdam, 1991; p 531.

(58) Dubois, J. L.; Fujieda, S. *Preprints of the 37th Congress of the Japan Petroleum institute*; Spring Meeting: Tokyo, May 18, 1994.

(59) Giellisse, P. J. M.; Foster, W. R. *Nature* **1962**, 195, 69.

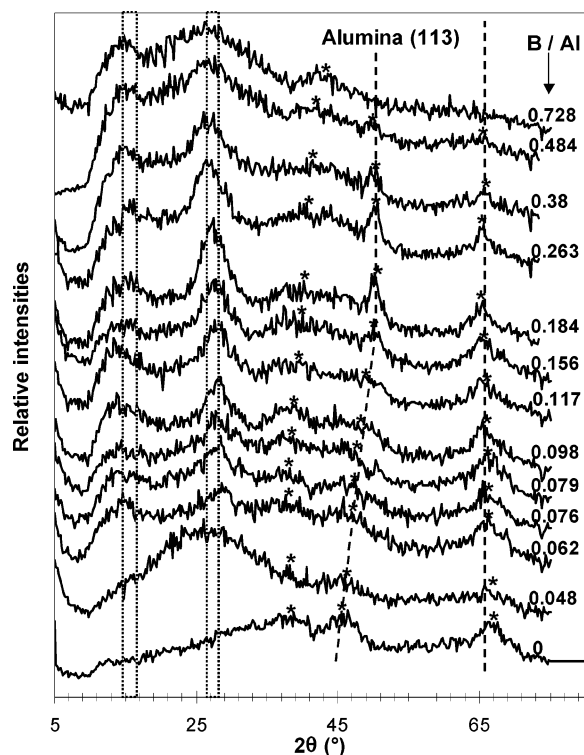


Figure 4. Diffractograms of the calcined samples.

Table 1. Main XRD Peaks Observed for Selected Boria and Boria–Alumina Mixed Compounds

compound	ASTM	main features (2θ) (relative intensity)				
B ₂ O ₃	13-0570	27.8° (100)	14.6° (35)	23.4° (25)		
H ₃ BO ₃	30-0199	28° (100)	14.6° (30)	15° (20)		
A ₂ B	47-0319	16.4° (100)	26.1° (78)	41.5° (51)		
A ₉ B ₂	32-0003	16.5° (100)	20.4° (50)	26.4° (40)	33.3° (40)	

peaks in the dotted rectangles could be either attributed to mixed oxides (A₉B₂, A₂B) or H₃BO₃ or B₂O₃ or a combination of them in a poorly crystallized state. Further, for B/Al = 0, the features are, as expected, characteristic of a poorly crystallized sol–gel γ -alumina.⁶⁰

The peak near $2\theta = 45^\circ$ corresponding to diffraction on the alumina (113) plane is shifted to higher angles when the boron loading increases up to the ratio B/Al ≈ 0.15 and then stabilizes at $2\theta \approx 50^\circ$. This is again the ratio of B/Al = 0.15 that seems to be a critical structural limit for the calcined oxides. The progressive shift of this peak suggests that, when boron is introduced, the host network is progressively modified to accept the BO₃ entities in its structure. Then, in the B/Al range from 0.15 to 0.38, the alumina (113) plane diffraction remains present at a constant 2θ value of about 50° , suggesting that a given mixed phase is present for the solids. As this mixed phase imposes constraints related to its genesis on the alumina lattice, the alumina peak is shifted, which is characteristic of an epitactic organization (A₉B₂- or A₂B-like phase might be formed over/through an Al₂O₃ framework). Then, for B/Al > 0.38 (beginning of domain IV of the xerogels), the alumina (113) plane peak is no more observable and the spectra are constituted essentially of very broad features that can be attributed to boria–alumina mixed

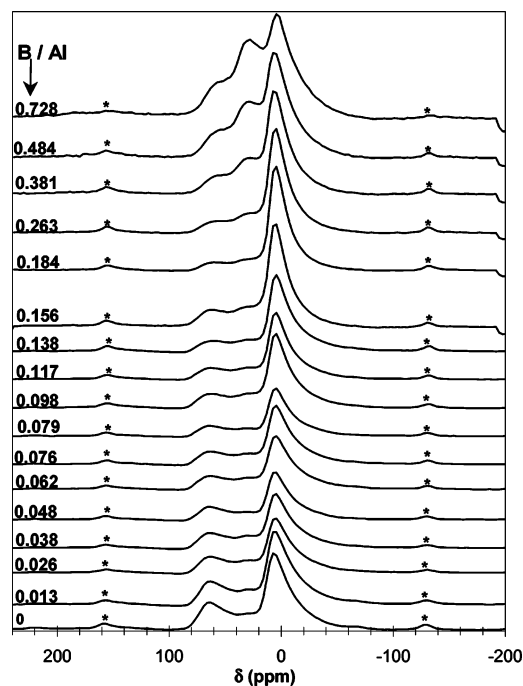


Figure 5. ²⁷Al NMR spectra of the calcined samples.

oxides. The solids have then not any more a pseudo-epitactic character but can be rather described as “real” bulk random mixed oxides.

NMR. The ²⁷Al NMR spectra of the calcined mixed oxides are presented in Figure 5. They are very different from those obtained for xerogels¹ with a remarkable increase in the intensity of the peaks attributed to tetrahedral (~ 60 ppm) and pentahedral (~ 40 ppm) aluminum species. Moreover, the spectra shape evolves sensibly with the boron loading. For B/Al atomic ratio between 0 and 0.184, the relative proportion of each species does not change significantly, while starting from B/Al = 0.263 a modification of the global shape of the spectra is observed with a drastic increase in the intensity of the peaks of tetrahedral and pentahedral aluminum species. It is remarkable to note that the spectra of high boron loadings samples are similar to that obtained for an A₉B₂ phase.⁶¹ Further, to check if the peak observed near 30 ppm is effectively due to pentahedral species and not to shifted tetrahedral species, a MQ-MAS spectrum of one selected sample has been recorded (Figure 6). This permitted to clearly identify the presence of pentahedral aluminum species according to a methodology described elsewhere.⁵⁶ This presence means that the peak near 30 ppm is not due to tetrahedral aluminum species which have been shifted by the proximity of boron atoms (B–O–Al bonds) as it was suggested by other authors for solids prepared by coprecipitation.¹² In addition, in the dried xerogel state, the creation of pentahedral aluminum species was also observed from B/Al = 0.26. Their presence was presumably a consequence of an extreme distortion of the system that could not be considered any more as a boehmite modified with B atoms but rather as a mixed oxide precursor. Then, calcination transformed this system into a more organized mixed

(60) Dumeignil, F.; Sato, K.; Imamura, M.; Matsubayashi, N.; Payen, E.; Hiromichi, S. *Appl. Catal., A* **2003**, *241* (1–2), 319.

(61) Dupree, R.; Holland, D.; Williams, D. S. *Phys. Chem. Glasses* **1985**, *26* (2), 50.

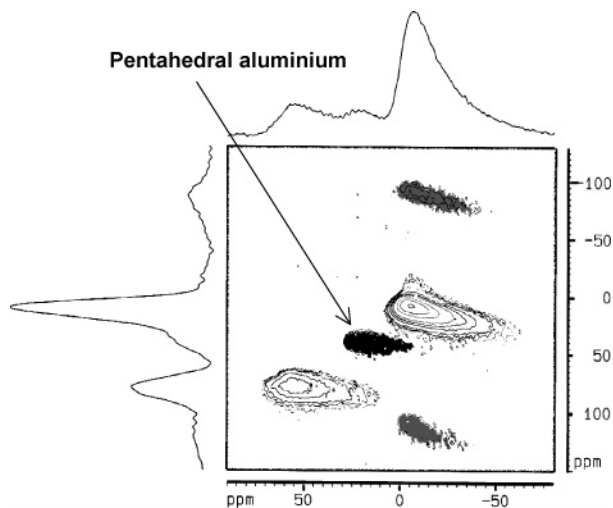


Figure 6. ^{27}Al MQMAS spectrum of one calcined sample ($\text{B}/\text{Al} = 0.138$).

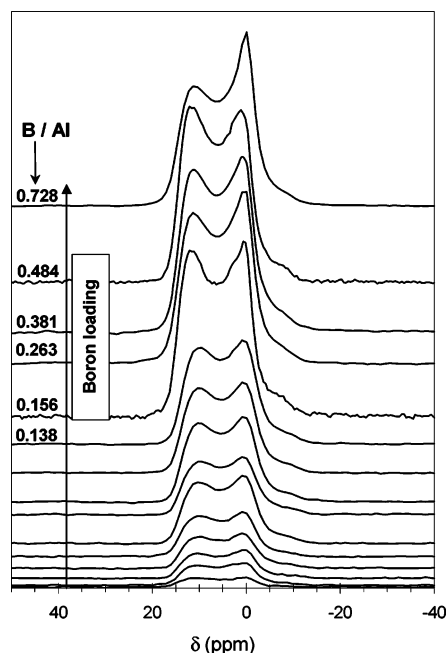


Figure 7. ^{11}B NMR spectra of the calcined samples.

oxide in which pentahedral aluminium species are more abundant.

The ^{11}B NMR spectra of the calcined mixed oxides are presented in Figure 7. Their shapes are also clearly different from those obtained for the dried xerogels.¹ Indeed, while on the dried xerogels a broad band with a small shoulder at low ppm was observed (BO_3 species and BO_4 species respectively), a doublet is observed in the calcined solids. For $\text{B}/\text{Al} \geq 0.263$, the low ppm peak exhibits clearly a sharp feature at its top part. As stated in the previous paper, the signal due to the BO_3 species was modified by a quadrupolar interaction. While in the case of the dried xerogels, this interaction intensity was not strong enough to generate an apparent splitting of the signal (only a broadening was observed), in the case of the calcined solids, the quadrupolar interaction becomes sufficiently strong to make apparent the peak splitting. The NMR spectra have been simulated and, as expected, the low ppm part of the BO_3 doublet contains a component due to BO_4 species. To reveal this feature, the spectra are first simulated with the QUASAR software in

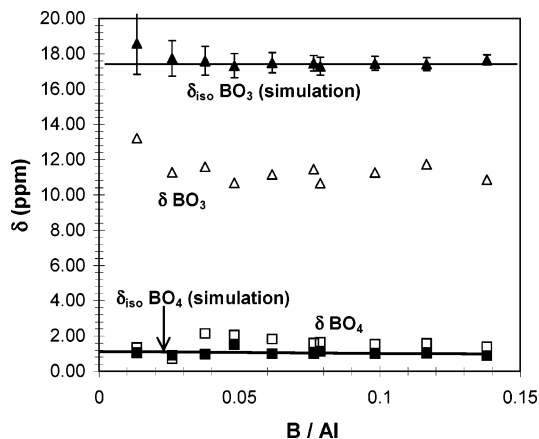


Figure 8. Observed and calculated boron chemical shift for calcined samples (low boron loadings).

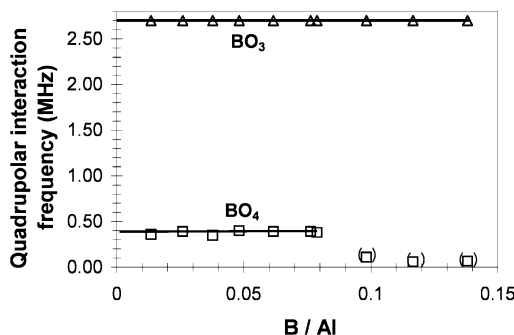


Figure 9. Quadrupolar interaction frequency for calcined solids (low boron loadings).

the same way as for the dried xerogels¹ considering only the presence of BO_3 species. For all the samples, a significant simulation misfit is always observed on the low ppm part of the simulated BO_3 doublet. Then, by subtracting each experimental spectrum with the corresponding BO_3 simulated spectrum, the peak due to BO_4 species is revealed and can be further separately simulated. Furthermore, the simulated parameters obtained separately for the BO_3 and the BO_4 components are subsequently input together to finely simulate each global spectrum and a difference equal to only $\pm 1\%$ is obtained for the new parameters when compared with the values obtained for the separated simulations. The simulations allow the determination of the quadrupolar interaction intensity and the real chemical shift of each species as well as the BO_4/BO_3 ratio. The results are presented and discussed separately for the low boron and the high boron loadings:

(i) Low Boron Loadings (Domains I and II of Xerogels).

The calculated “true” chemical shifts of the boron species are modified after calcination when compared with those obtained for the corresponding dried xerogels.¹ The chemical shift of the BO_3 species increased from 16 to 17.5 ppm when the dried xerogels were calcined, while it decreased in the same time from 2 to 1.1 ppm for the BO_4 species (Figure 8). In addition, the quadrupolar interaction on the BO_3 species increased from 2.3 MHz (dried xerogels) to 2.7 MHz upon calcination (Figure 9), which reflects an increase in the distortion of the local environment of the BO_3 species that are compelled to fit up in an organized oxide structure. For the BO_4 species, the quadrupolar interaction is about 0.4 MHz up to about $\text{B}/\text{Al} = 0.08$ and then seems to become very

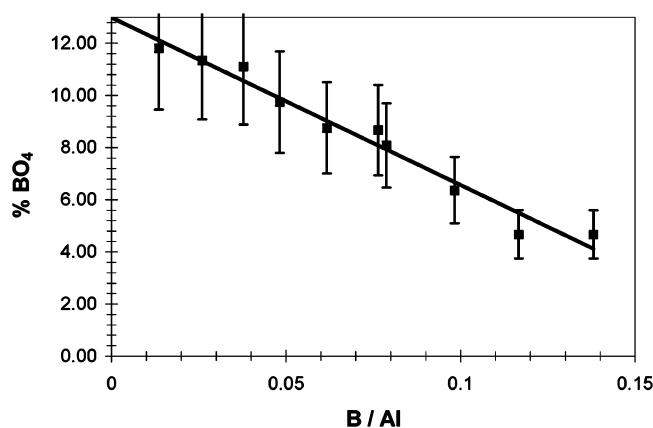


Figure 10. Percent BO_4 defined as $\{B(\text{BO}_4)\}/[B(\text{BO}_4) + B(\text{BO}_3)] \times 100$ on calcined solids (low boron loadings).

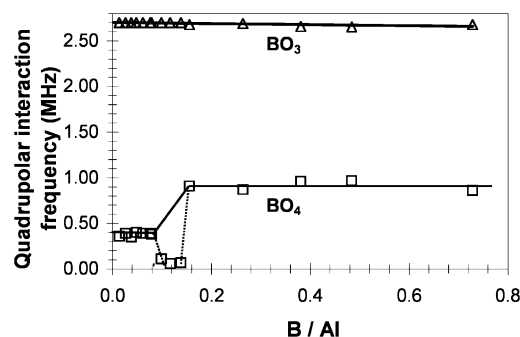


Figure 11. Quadrupolar interaction frequency for boron species and for all the boron loadings.

small. In fact for $0.08 < B/Al < 0.15$, the BO_4 species quantity is quite low (Figure 10) and the simulation misfit is not sensitive to the quadrupolar interaction intensity applied on the BO_4 species signal in a reasonable range. Then, the simplex algorithm converges artificially to a value close to 0. Forcing the software to apply a value of 0.4 MHz did not change significantly the results when simulating the spectra of the solids with $0.08 < B/Al < 0.15$. Therefore, the variations of the quadrupolar interaction intensity as a function of the B/Al atomic ratio in the full range of studied compositions are arbitrarily linked (Figure 11). The value of 0.4 MHz obtained for the low boron loadings is in good agreement with the value extrapolated for “isolated” BO_4 species ($\text{Al}-(\text{OAl})_3\text{BO}_4$ species) in the dried xerogels.¹

(ii) High Boron Loadings (Domains III and IV of the Dried Xerogels). For high loadings, the quadrupolar interaction on the BO_3 species remains constant at about 2.7 MHz (for $B/Al > \sim 0.15$ in Figure 11). In contrast, the quadrupolar interaction on the BO_4 species increases from 0.4 to 0.9 MHz for $B/Al = 0.15$ (which corresponds again to the interface between the domains II and III of the dried xerogels). From $B/Al = 0.15$, the dried xerogels started to be crossed by BO_3 chains that became sufficiently long, and as aforementioned, it is well known that BO_3 species organized in chains can volatilize at relatively low temperatures.^{14,57,58} According to Giellise et al. (Figure 2), the temperature of fusion of B_2O_3 is about 450 °C; further, Handbook of Chemistry and Physics⁶² indicates that the ebullition temperature of this

compound is of about 1860 °C. Although no numerical values were found for the B_2O_3 superficial vapor tension, Maljuk et al.⁶³ annealed pure B_2O_3 in an Al_2O_3 crucible at 1240 °C (12 h, air) and found that the volatility of boron oxide was equivalent to nearly 1.2 wt % per day. This suggests that volatilization of well-crystallized boron oxide is not so effective. Nevertheless, in our case, two points have to be taken into consideration: (i) we are not in the presence of a well-defined B_2O_3 structure but rather in the presence of BO_3 chains more or less dissolved into a boehmite matrix; (ii) the system is calcined from the dried state, which means that it is not yet so well organized into a real mixed oxide and thus very unstable. Then, evaporation of boron oxide might occur at the earlier stage of calcination procedure for which the oxidic species entanglement is not so structured and thus can be easily subjected to heat decompositions. Further, boehmite conversion into alumina involves structure reorganization with H_2O molecules liberation. In addition, Buyevskaya et al.⁶⁴ who studied partial oxidation of propane over boria–alumina proposed that the observed activity decrease with the time on stream was due to volatilization of BO_3 species during the reaction and their conversion into boric acid due to the presence of H_2O in the feed gas. This is in good agreement with our assumption. Then, considering the B/Al composition results (loss of boron upon calcination, Figure 1) and the increase in the SSA (Figure 3) starting at $B/Al = 0.15$, the morphological change induced by calcination with volatilization of (a part of) BO_3 chains can be schematically illustrated in Figure 12 on which dislocation of the boehmite sheets is presented. Before calcination, surface BO_4 species are present on the top parts of the sheets of the host boehmite structure and it can be supposed that most of them are likely to remain after calcination (and rehydration). After calcination, some BO_3 species that were in the inner part of the matrix (hatched triangles in Figure 12a) are now on the top of the newly created surfaces and can therefore undergo hydration and become BO_4 species. As these latter BO_4 species were inner BO_3 species in the xerogel, they might be still strongly strained in the new surface layer (epitactic growth as discussed from the XRD results). Therefore, their local environment is different from the one of the initial BO_4 species. These latter species exhibited a quadrupolar interaction intensity of about 0.4 MHz, and the creation of the new type of BO_4 species from $B/Al > 0.15$ is responsible for an increase in the apparent global quadrupolar interaction intensity up to about 0.9 MHz. Further, as for the dried xerogels, the BO_3 chemical shift do not seem to be significantly modified when the B/Al ratio changes (Figure 13). In contrast, the simulated chemical shift of the BO_4 species peak seems to slightly increase from $B/Al = 0.15$, which is in good agreement with the above discussion. Indeed, it is very likely that most part of the BO_4 species for $B/Al > 0.15$ are not of the same type as the ones for $B/Al < 0.15$.

(63) Maljuk, A.; Watauchi, S.; Tanaka, I.; Kojima, H. *J. Cryst. Growth* **2000**, 212, 138.

(64) Buyevskaya, O. V.; Müller, D.; Pitsch, I.; Baerns, M. *Stud. Surf. Sci. Catal.* **1998**, 119, 671.

(62) *Handbook of Chemistry and Physics*, 66th ed.; CRC Press Inc.: Boca Raton, FL, 1985–1986.

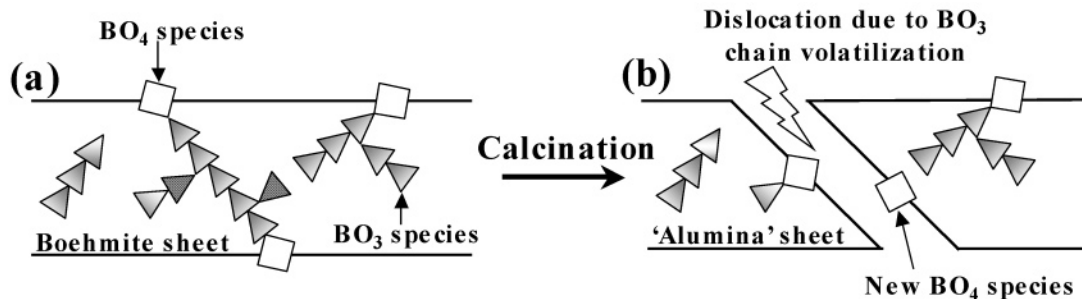


Figure 12. Schematic representation of a sheet of boehmite host structure (xerogel) and of the same sheet after calcination (γ -alumina sheet) for $B/Al > 0.15$.

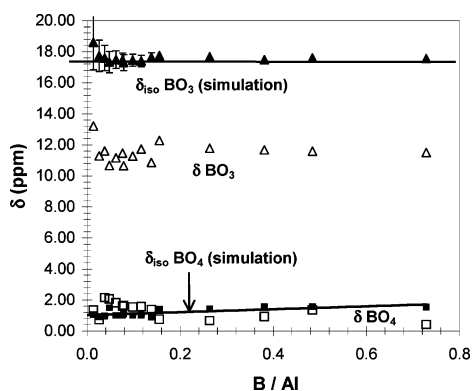


Figure 13. Chemical shifts of boron species in the calcined solids.

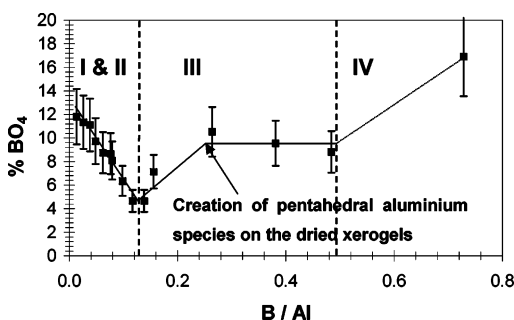


Figure 14. Percent BO_4 defined as $\{B(BO_4)\}/\{B(BO_4) + B(BO_3)\} \times 100$ on calcined solids (full range of boron loadings).

Finally, Figure 14 presents the BO_4 species quantity as a function of the B/Al atomic ratio. Three parts can be distinguished. In the first part, corresponding to domains I and II of the dried xerogels, the BO_4 percentage decreases linearly. In the second part, from $B/Al \approx 0.13$ to $B/Al \approx 0.50$, which corresponds substantially to domain III of the dried xerogels, the BO_4 species percentage increases up to $B/Al \approx 0.26$ and then stabilizes from $B/Al \approx 0.26$ to $B/Al \approx 0.50$. Finally, in the third part, corresponding to domain IV of the dried xerogels, the percentage of BO_4 species increases drastically. These values, limiting the different composition parts, are in good agreement with the values of the Giellisse et al. diagram⁵⁹ (Figure 2). Indeed, according to this diagram, while alumina and the A_9B_2 phase are formed for $0 < B/Al < 0.18$, for $0.18 < B/Al < 0.43$ the two A_9B_2 and A_2B phases coexist and for $B/Al > 0.43$, B_2O_3 and the A_2B phase are both present. Furthermore, these limits are also in very good agreement with the XRD results, i.e., that the alumina is first modified by the presence of inner BO_3 chains for $0 < B/Al < \approx 0.15$ and then for $B/Al > 0.15$ an epitactic-like mixed oxide phase is progressively created.

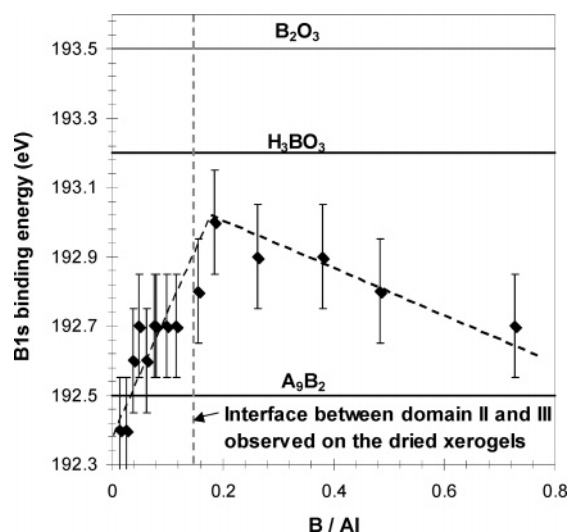


Figure 15. Binding energy of B 1s level as a function of the bulk B/Al ratio.

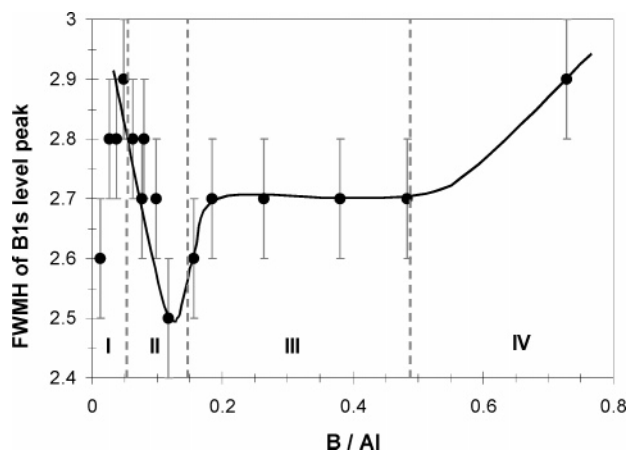


Figure 16. Evolution of the fwhm of the B 1s level peak as a function of the bulk B/Al ratio.

Then, for $B/Al > 0.381$, the system loses totally its “alumina-like” character as the alumina XRD features completely disappear from the diffractograms.

XPS. Figure 15 represents the XPS binding energy of the B 1s core level as a function of the bulk B/Al ratio while Figure 16 represents evolution of its full width at half-maximum (fwhm). The binding energies reported in Figure 15 are calculated by reference to the Al 2p level at 74.8 eV, the value generally obtained for γ -alumina. As a remark, the observed O 1s binding energy is constant at a value of

531.9 \pm 0.1 eV, the fwhm being of 3.3 \pm 0.1 eV irrespective of the B/Al ratio. As observed in Figure 15, up to B/Al = 0.18, a value which is close to the transition between domains II and III observed on the dried xerogels, the B 1s binding energy increases quite linearly and then decreases progressively for higher B/Al ratios. For low B/Al ratios, boron is supposed to be randomly dispersed in the alumina matrix, meaning that a mixed phase is locally formed, in good agreement with the Gielisse et al. diagram (Figure 2). Therefore, the observed binding energy for very low B/Al ratios (\sim 192.4–192.6 eV, Figure 15) is close to the one of a model A_9B_2 phase (192.5 eV). Then, for B/Al > 0.05, BO_3 chains progressively developed in the dried xerogels and a part of them remained after calcination. Therefore, the BO_3 species are locally more and more surrounded by other BO_3 entities, as is the case for H_3BO_3 or B_2O_3 solids that contain exclusively BO_3 chains. Thus, the B 1s binding energy progressively increases when increasing the B/Al ratio up to about 0.2 with a value of 193 eV, to be compared with the value commonly observed for H_3BO_3 (193.2 eV) or B_2O_3 (193.5 eV). Further for B/Al > 0.15, as represented in Figure 12, calcination induces cleavage caused by volatilization of BO_3 chains sufficiently long for crossing the boehmite matrix. Then, new B oxo-species are created on the new surfaces (hatched species in Figure 12). In other words, for B/Al > 0.15, the system becomes progressively a “real” mixed phase with B and Al species “randomly” distributed at the particle level. Consequently, the B 1s binding energy progressively decreases to approach again the value observed for an A_9B_2 phase (192.5 eV) when B/Al increases.

The shape of Figure 16 (fwhm of the B 1s peak) is very similar to the one obtained for the calculated percentage of BO_4 (Figure 14), and it is then likely that the fwhm is influenced by the percentage of BO_4 in the solids. Indeed, while the XPS resolution is not sufficient to separate the peaks of the different B species, the B 1s peak appears more or less broadened due to a certain distribution in the binding energies of the respective species. Moreover, unlike the case of the NMR spectra that have been recorded at atmospheric pressure without any pretreatment (except for the experiment used to verify the disappearance of the BO_4 peak after dehydration; a result not shown here), the XPS spectra are taken after degassing the samples under very low pressures, and the BO_4H species are converted into BO_3 species by dehydration prior to the measurement. Therefore, the observed binding energies are the ones of bulk BO_3 species and surface BO_3 species (that can undergo the aforementioned hydration/dehydration process). As their environment differs only slightly, their binding energy might be therefore rather close, unlike if the surface ones were BO_4 species (electronic influence of the fourth oxygen atom). This slight difference is reflected in the fwhm of the peak. This result is in very good agreement with the QUASAR simulations results. It appears interesting to note that modification of the local environment of atoms which induces changes in the binding energy of core level(s) has already been reported in the literature for mixed oxides other than boria–alumina. For example, the Ti 2p_{3/2} line shifts from 458.5 eV for Ti in octahedral coordination as in TiO_2 to about 460.0 eV for Ti

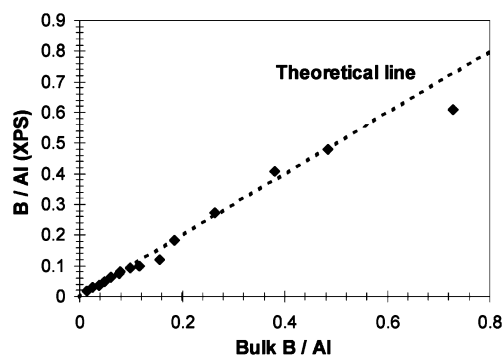


Figure 17. B/Al ratio as determined by XPS as a function of the B/Al bulk ratio.

in tetrahedral coordination in mixed TiO_2 – SiO_2 aerogels with low Ti content. In the latter case, the Ti atoms are mainly surrounded by O–Si linkages.⁶⁵

Finally, to check about the homogeneity of the solids, the B/Al ratios are calculated from the XPS results using the three-dimensional-thick binary oxide model described elsewhere.⁵⁵ In this model, calculations of atomic ratio from XPS are obtained by integrating the differential equation relative to the XPS intensity of a given line vs the position in the solid of atoms emitting photoelectrons from 0 (uppermost surface layer) to ∞ (sample “thick” relative to the mean free path of the photoelectrons). Such an investigation permits to probe elements in a solid depth to about 10 nm. The fact that the B/Al calculated ratio from XPS peak intensity [B/Al (XPS)] are very close to bulk ratio as measured by X-ray fluorescence (Figure 17) indicates that the samples of that system exhibit a good B–Al homogeneity: the B/Al surface ratio (0–10 nm) is representative of the B–Al bulk ratio.

Conclusions

The calcined boria–alumina mixed oxides with different B/Al atomic ratios have been characterized by various complementary techniques that show consistent results, further validating a fortiori the model proposed for the corresponding dried xerogels.

For B/Al < 0.15, the solids are composed of a γ -alumina host matrix locally modified with BO_3 species. The random distribution of BO_3 species modifies progressively the alumina original network, and the XRD peak attributed to the (113) plane of γ -alumina progressively shifts to higher 2θ when B/Al increases.

For B/Al > 0.15, the structure of the solids drastically changes. Indeed, in the corresponding dried xerogels, BO_3 chains are developing and progressively cross the host matrix. The sufficient long BO_3 chains are (partly) volatilized during calcination, and the measured B/Al ratio of the calcined oxides become significantly lower than the theoretical one, while in contrast an excellent correlation is obtained for B/Al < 0.15. Volatilization of the BO_3 chains leads to a dislocation of the initial system, and the specific area of the solids increases noticeably for calcined samples with B/Al higher than 0.15. Then, new exposed surfaces are created, which exhibit boron oxo-species that were previously members of

(65) Beck, C.; Mallat, T.; Burgi, T.; Baiker, A. *J. Catal.* **2001**, *204*, 438.

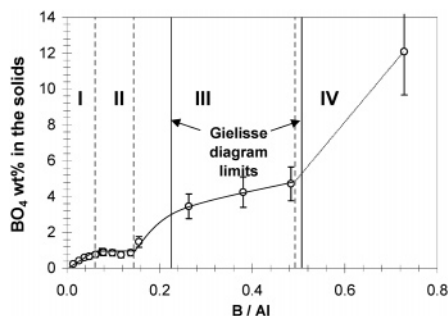


Figure 18. Amount of boron in tetrahedral coordination calculated in BO_4 wt % in $\text{B}-\text{Al}_2\text{O}_3$ as a function of the B/Al ratio.

core BO_3 chains. The creation of these new BO_3 species (hydrated into BO_4 species in the ambient atmosphere) that are incrustated in the surface of the solids is accompanied with an increase in the quadrupolar interaction intensity (calculated by simulating the ^{11}B MAS NMR spectra) observed on the BO_4 species. When the longer BO_3 chains have been volatilized, the B remaining oxo-species are well distributed in the network with supposedly a non-negligible part incrustated in the cleaved surface. The solids can then be considered as mixed phases according to the following arguments:

(1) The XPS results have shown that for $\text{B}/\text{Al} < 0.15$ the B 1s binding energy progressively increases with the boron loading (organization into longer and longer BO_3 chains), while for $\text{B}/\text{Al} > 0.15$ it progressively decreases to become closer and closer from the B 1s binding energy observed for a mixed $9\text{Al}_2\text{O}_3 \cdot 2\text{B}_2\text{O}_3$ phase.

(2) The shape of the ^{27}Al MAS NMR spectra becomes similar to the one obtained in previous literature for the above-mentioned $9\text{Al}_2\text{O}_3 \cdot 2\text{B}_2\text{O}_3$ phase, especially for $\text{B}/\text{Al} > 0.184$.

(3) The XRD diffractograms progressively lose the features of γ -alumina, especially for $\text{B}/\text{Al} > 0.263$, while the shift of the peak due to the diffraction on the (113) plane of the γ -alumina stops from $\text{B}/\text{Al} \sim 0.156$, indicating the formation of a defined mixed phase (supposedly epitactic-like growth).

Further, the software simulations allowed to calculate the ratio BO_4/BO_3 (ratio between “surface BO_3 species” and “bulk BO_3 species”). Results are in good agreement with the creation of new exposed surfaces from $\text{B}/\text{Al} = 0.15$. In addition, the wt % of BO_4 species in the oxides as a function of the B/Al ratio is reported in Figure 18. It is remarkable that the limits that can be distinguished are in excellent agreement with either the limits defined for the dried xerogels and also of the phase diagram previously proposed by Gielisse et al.⁵⁹ As a final remark, the quantity of BO_4 species is a very important parameter. Indeed, as discussed above, these species are surface species and therefore boron species

that are accessible to molecules in the case of catalytic reactions. Further, the presence of BO_3 chains is also a very important parameter in the point of view of catalytic applications. Indeed, while these chains can volatilize for rather low temperatures, possibly leading to a loss of the properties initially brought by the B atoms in the system, it is also known that the catalytic system can autorepair by replenishment through the migration of the bulk B species to the solid surface.⁵⁸ Thus, to avoid undesirable volatilization of the active species while keeping the autoreparation property, it seems preferable to work with solids that contain reasonably short BO_3 chains. In other words, mixed oxides with rather well distributed boron species might be good candidates. By consideration of the solids of the present study, for $\text{B}/\text{Al} < 0.15$, short BO_3 matrix chains are present and might be volatilized for sufficient times on stream during catalytic applications. In contrast, for $\text{B}/\text{Al} > 0.15$, the solids progressively tend to exhibit the structure of mixed oxides, especially for $\text{B}/\text{Al} = 0.381, 0.484$, and particularly for 0.728 for which characteristic ^{27}Al MAS NMR spectrum features are obtained. Actually, some of the solids presented in this work have been used for example as catalysts for the vapor-phase Beckmann rearrangement of the cyclohexanone-oxime.⁶⁶ The results fit very well with the conclusions of the present study as the catalyst with $\text{B}/\text{Al} = 0.728$ exhibits a lifetime about twice higher than that of the ones with $\text{B}/\text{Al} = 0.013, 0.062$, and 0.280. In addition, the sol-gel boria-alumina catalysts showed longer lifetimes than those of solids prepared by conventional impregnation. This can be attributed to a higher stability of the boron species within the catalyst structure (BO_4 species incrustated in the cleaved surfaces). Furthermore, in another study boria-alumina carriers prepared using the method proposed in the present work have been subsequently impregnated with solutions containing Co and Mo species and then submitted to a sulfidation procedure to use them as HDS catalysts.⁶⁷ Thiophene and dibenzothiophene hydrodesulfurization reactions exhibited a maximum for $\text{B}/\text{Al} \approx 0.05$ (corresponding to end of domain I of the xerogels), for which a local maximum of acidity was observed by NH_3 adsorption/desorption experiments on the bare oxide carriers.

Acknowledgment. The authors want to thank the European Community, which has funded this work through the Joule III Project No. JOF3-CT95-0002.

CM048079K

- (66) Forni, L.; Fornasari, G.; Tosi, C.; Trifirò, F.; Vaccari, A.; Dumeignil, F.; Grimblot, J. *Appl. Catal., A* **2003**, *248*, 47.
 (67) Dumeignil, F.; Sato, K.; Imamura, M.; Matsubayashi, N.; Payen, E.; Shimada, H. in preparation, to be submitted to *Appl. Catal., A* **2005**.